ANL/ET/CP--85028
Conf-950695--1

FLOW-INDUCED VIBRATION OF TUBES IN CROSSFLOW*

S. S. Chen, Y. Cai and S. Zhu

Energy Technology Division

Argonne National Laboratory

Argonne, Illinois 60439

RECEIVED
JUN 1 9 1995
OSTI

To be submitted for presentation at the 14th International Conference on Offshore Mechanics & Arctic Engineering, June 18-22, 1995, Copenhagen, Denmark.

*This work was funded by the U. S. Department of Energy, Office of Basic Energy Sciences, Division of Engineering and Geosciences, under Contract W-31-109-Eng-38.

DISCLAIMER

Portions of this document may be illegible in electronic image products. Images are produced from the best available original document.

FLOW-INDUCED VIBRATION OF TUBES IN CROSSFLOW*

S. S. Chen, Y. Cai and S. Zhu
Energy Technology Division
Argonne National Laboratory
Argonne, Illinois 60439

Abstract

This paper presents an unsteady flow theory for flow-induced vibration of tubes in crossflow. It includes a general description of motion-dependent fluid forces, characteristics of fluid-force coefficients, and mathematical models. The detailed results are presented for the constrained mode in the lift direction for various tube arrangements.

1. Introduction

Various mathematical models have been developed to predict flow-induced vibration and instability of tubes subject to crossflow (Chen 1987, Price 1993). At this time, a number of issues have not been answered and several aspects of the problems have not been resolved. This paper is to present an unified theory for linear and nonlinear response of tubes in crossflow.

One of the key elements is the motion-dependent fluid forces. A water channel is used to measure fluid forces on all tubes due to the motion of a tube. From the measured fluid forces, fluid damping and stiffness for various tube arrays are obtained. Tests have been performed for a single tube, two tubes, and tube rows. These coefficients depend on reduced flow velocity, tube arrangement, oscillation amplitude, and Reynolds number. Some general characteristics of these fluid-force coefficients are observed.

Once fluid-damping and fluid-stiffness coefficient matrices are know, a mathematical model simulating practical tube arrays can be established and analyzed. The unsteady flow theory based on the measured fluid forces can be used to study the detailed tube motions, including subcritical vibration, instability threshold, and post-instability oscillations. It can also be used to assess the applicable ranges of other simplified theories such as quasistatic and quasisteady flow theories. Although fluid-force coefficients can not be obtained easily, the unsteady flow theory can describe the motion in detail.

The unsteady flow theory has also been applied to study the nonlinear vibration of loosely supported tube arrays. Tube displacements were analyzed to characterize the tube behavior by RMS values, power spectral densities, phase planes, Poincare maps, Lyapunov exponents, and fractal dimension. The analytical results and experimental agree reasonably well (Cai and Chen 1993; Chen, Zhu, and Cai 1994). This demonstrates the usefulness of the unsteady flow theory.

This paper presents an unsteady flow theory to study the import practical problems with academic interest. It includes measurement of fluid damping and stiffness, and mathematical model for tube vibration. Details are presented for a single flexible tube in a rigid tube array. The general theory is applicable for an array of elastic tubes.

2. Unsteady-Flow Theory of Motion-Dependent Fluid Forces

Consider a tube oscillating in a rigid tube array (see Fig. 1). The fluid is flowing with a flow velocity U. The displacement components of the tube in the x and y directions (or lift and drag directions) are u and v, respectively. The motion-dependent fluid-force components acting on the tube in the x and y directions are f and g, respectively, which can be written as (Chen 1987)

$$f = -\rho\pi R^2\left(\alpha\frac{\partial^2 u}{\partial t^2}+\sigma\frac{\partial^2 v}{\partial t^2}\right)+\frac{\rho U^2}{\omega}\left(\alpha'\frac{\partial u}{\partial t}+\sigma'\frac{\partial v}{\partial t}\right)+\rho U^2(\alpha'' u+\sigma'' v) \tag{1}$$

$$g = -\rho\pi R^2\left(\tau\frac{\partial^2 u}{\partial t^2}+\beta\frac{\partial^2 v}{\partial t^2}\right)+\frac{\rho U^2}{\omega}\left(\tau'\frac{\partial u}{\partial t}+\beta'\frac{\partial v}{\partial t}\right)+\rho U^2(\tau'' u+\beta'' v), \tag{2}$$

where ρ is fluid density, R is tube radius, t is time, and ω is circular frequency of tube oscillation. α, β, σ, and τ are added mass coefficients, α', β', σ', and τ' are fluid-damping coefficients, and α'', β'', σ'', and τ'' are fluid-stiffness coefficients.

Various methods can be used to measure fluid-force coefficients (Chen, Zhu, and Jendrzejczyk 1994). In this study, the unsteady-flow theory was used. Fluid-force coefficients can be determined by measuring the fluid forces acting on the tube because of its oscillations. For example, if the tube is excited in the y direction, its displacement in the y direction is given by (u = 0)

$$v = v_0 \cos \omega t. \tag{3}$$

The fluid force acting on the cylinder in the x direction can be written

$$f = \frac{1}{2}\rho U^2 c \cos(\omega t + \phi) v_0, \tag{4}$$

where c is the fluid-force amplitude and ϕ is the phase angle by which the fluid force acting on the tube leads to displacement of the tube.

With Eqs. 1 and 3, we can also write the fluid-force component as

$$f = \left(\rho\pi R^2\omega^2\sigma + \rho U^2\sigma''\right)v_0 \cos\omega t - \rho U^2\sigma' v_0 \sin\omega t. \tag{5}$$

By combining Eqs. 4 and 5, we obtain

$$\sigma'' = \frac{1}{2} c \cos\phi - \frac{\pi^3}{U_r^2}\sigma \tag{6}$$

and

$$\sigma' = \frac{1}{2} c \sin\phi, \tag{7}$$

where U_r is the reduced flow velocity ($U_r = \pi U/\omega R$).

The added mass coefficient σ in Eq. 6 can be calculated by applying the potential-flow theory (Chen 1975 and 1987). The values of σ' and σ'' can be calculated from Eqs. 6 and 7 when the force amplitude c and phase angle ϕ are measured. Fluid-force coefficients α', α'', β', β'', τ', and τ'' can be obtained in the same manner.

Fluid-force coefficients depend on the arrangement and pitch, oscillation amplitude and frequency, and flow velocity. For a given tube arrangement, fluid-force coefficients are a function of oscillation amplitude (d/D) and reduced flow velocity (U_r) and Reynolds number, where d is vibration amplitude and D is cylinder diameter. For small-amplitude oscillations and large Reynolds number, fluid-force coefficients can be considered a function of reduced flow velocity only.

3. Measuring Fluid-Force Coefficients

A water channel was used to measure motion-dependent fluid forces. The test setup and measurement technique are presented by Chen, Zhu, and Jendrzejczyk (1994).

In this paper, the following cases are presented (Fig. 2):

a. A single tube.

b. Two tubes in tandem with a pitch to diameter ratio of 1.35.

c. A tube in the wake of another tube.

d. Two tubes normal to flow with a pitch to diameter ratio of 1.35.

e. A tube row with a pitch to diameter ratio of 2.7.

f. A tube row with a pitch to diameter ratio of 1.35.

In each test, the excitation frequency ranges from about 0.2 to 2.2 Hz and the flow velocities vary from about 0.05 to 0.17 m/s. The Reynolds number varies from about 1200 to 4200.

Note that in Eqs. 1 and 2, α' and β', and α'' and β'' are self fluid-damping and stiffness coefficients associated with the fluid forces induced in the same direction as tube oscillations. σ' and τ', and σ'' and τ'' are mutual fluid-damping and fluid-stiffness coefficients associated with the fluid forces perpendicular to tube oscillations. In addition, when one tube is excited, motion-dependent fluid forces on the surrounding tubes are also induced (Chen, Zhu, and Jendrzejczyk 1994). In this paper these forces are not presented.

Fluid-damping coefficients α', β', σ', and τ', and fluid-stiffness coefficients, α'', β'', σ'', and τ'', are obtained for all cases, see Fig. 2. To limit the length of this paper, only the data for α' and α'' are presented:

- Fig. 3: α' and α'' for a single tube at a flow velocity equal to 0.127 m/s for various rms excitation amplitude, d.

- Fig. 4: α' and α'' for two tubes in tandem at three flow velocities, 0.07, 0.11 and 0.15 m/s (Ug is gap flow velocity).

- Fig. 5-7: α' and α'' for a tube in the wake of another for three pitch-to-diameter ratios at a flow velocity of 0.11 m/s and various rms excitation amplitude, d.

- Fig. 8: α' and α'' for two tubes normal to flow with T/D = 1.35 for a series of gap flow velocities (Ug), 0.05, 0.07, 0.113, 0.146, and 0.166 m/s.

- Figs. 9 and 10: α' and α'' for tube rows with T/D = 1.35 and 2.7 for various rms excitation amplitude, d.

From Figs. 3-10 and other data not presented in this paper, some general characteristics of motion-dependent fluid-force coefficients are noticed:

- Reynolds Number: At low reduced flow velocity, fluid-force coefficients depend on the reduced flow velocity, Reynolds number, and excitation amplitude. This can be seen from the results given in Figs. 3-10.

- High Reduced Flow Velocity: When the reduced flow velocity is high, e.g., >20 and some >10, all fluid-force coefficients are approximately independent of reduced flow velocity. This characteristic is not only valid for circular cylinders, but also for other geometries (Chen and Chandra 1991).

- Drastic changes in the fluid-force coefficients occurred in the region corresponding to vortex shedding for a single cylinder and tube rows. In the critical region, the magnitudes of the coefficients also depended on the excitation amplitude.

4. Mathematical Model for Flow-Induced Vibration

Once fluid-excitation and motion-dependent fluid forces are known, the response of the tube can be predicted. Consider an elastic tube in a rigid tube array with radius R (= D/2) (Fig. 1). The variables associated with the motion of the elastic tube in the x and y directions are flexural rigidity EI, tube mass per unit length m, structural damping coefficient C_s, and displacements u and v. The equations of motion for the tube in the x and y directions , respectively, are (Chen 1987)

$$EI\frac{\partial^4 u}{\partial z^4}+C_s\frac{\partial u}{\partial t}+m\frac{\partial^2 u}{\partial t^2}+\rho\pi R^2\left(\alpha\frac{\partial^2 u}{\partial t^2}+\sigma\frac{\partial^2 v}{\partial t^2}\right)$$

$$-\frac{\rho U^2}{\omega}\left(\alpha'\frac{\partial u}{\partial t}+\sigma'\frac{\partial v}{\partial t}\right)-\rho U^2(\alpha'' u+\sigma'' v)=g'(t) \tag{8}$$

and

$$EI\frac{\partial^4 v}{\partial z^4}+C_s\frac{\partial v}{\partial t}+m\frac{\partial^2 v}{\partial t^2}+\rho\pi R^2\left(\tau\frac{\partial^2 u}{\partial t^2}+\beta\frac{\partial^2 v}{\partial t^2}\right)$$

$$-\frac{\rho U^2}{\omega}\left(\tau'\frac{\partial u}{\partial t}+\beta'\frac{\partial v}{\partial t}\right)-\rho U^2(\tau'' u+\beta'' v)=h'(t), \tag{9}$$

where g'(t) and h'(t) are forced excitations. Note that the fluid-damping and -stiffness coefficients are functions of reduced flow velocity U_r.

The in-vacuum variables are mass per unit length m, modal damping ratio ζ_v ($C_s/2m\omega_v$), and natural frequency f_v ($=\omega_v/2\pi$). The values for f_v and ζ_v can be calculated from the equation of motion and appropriate boundary conditions or from tests in vacuum (practically in air). The modal function $\varphi(z)$ of a cylinder vibrating in vacuum and in fluid is

$$\frac{1}{\ell}\int_0^{\ell}\varphi^2(z)dz = 1, \tag{10}$$

where ℓ is the length of the cylinder. Let

$$u(z,t) = a(t)\varphi(z)$$

and (11)

$$v(z,t) = b(t)\varphi(z),$$

where a(t) and b(t) are functions of time only. Calculation of Eqs. 8 and 9 yields, respectively,

$$\ddot{a} + \gamma\left(\alpha\ddot{a} + \sigma\ddot{b}\right) + 2\zeta_v\omega_v\dot{a} - \frac{\gamma}{\pi^3}U_v^2\left(\frac{\omega_v^2}{\omega}\right)\left(\alpha'\dot{a} + \sigma'\dot{b}\right)$$

$$+\omega_v^2 a - \frac{\gamma}{\pi^3}U_v^2\omega_v^2(\alpha''a + \sigma''b) = f \tag{12}$$

and

$$\ddot{b} + \gamma\left(\tau\ddot{a} + \beta\ddot{b}\right) + 2\zeta_v\omega_v\dot{b} - \frac{\gamma}{\pi^3}U_v^2\left(\frac{\omega_v^2}{\omega}\right)\left(\tau'\dot{a} + \beta'\dot{b}\right)$$

$$+\omega_v^2 b - \frac{\gamma}{\pi^3}U_v^2\omega_v^2(\tau''a + \beta''b) = g, \tag{13}$$

where

$$
\begin{aligned}
U_v &= \frac{U}{f_v D} \\
\gamma &= \frac{\rho \pi R^2}{m} \\
g &= \frac{1}{m\ell}\int_0^\ell f'\,\phi(z)dz \\
h &= \frac{1}{m\ell}\int_0^\ell g'\,\phi(z)dz.
\end{aligned}
\tag{14}
$$

The dot denotes differentiation with respect to time. Natural frequencies, modal dampings, and tube response can be calculated from Eqs. 12 and 13; i.e., can be written as

$$[M]\ddot{q} + [C]\dot{q} + [K]q = p, \tag{15}$$

where

$$q = \begin{Bmatrix} q_1 \\ q_2 \end{Bmatrix} = \begin{Bmatrix} a \\ b \end{Bmatrix},$$

$$p = \begin{Bmatrix} g \\ h \end{Bmatrix},$$

$$[M] = \begin{pmatrix} 1+\gamma\alpha & \sigma \\ \tau & 1+\gamma\beta \end{pmatrix},$$

$$[C] = \begin{bmatrix} 2\zeta_v\omega_v - \frac{\gamma}{\pi^3}U_v^2\left(\frac{\omega_v^2}{\omega}\right)\alpha' & -\frac{\gamma}{\pi^3}U_v^2\left(\frac{\omega_v^2}{\omega}\right)\sigma' \\ -\frac{\gamma}{\pi^3}U_v^2\left(\frac{\omega_v^2}{\omega}\right)\tau' & 2\zeta_v\omega_v - \frac{\gamma}{\pi^3}U_v^2\left(\frac{\omega_v^2}{\omega}\right)\beta' \end{bmatrix}, \tag{16}$$

and

$$[K] = \begin{pmatrix} \omega_v^2 - \frac{\gamma}{\pi^3}U_v^2\omega_v^2\alpha'' & -\frac{\gamma}{\pi^3}U_v^2\omega_v^2\sigma'' \\ -\frac{\gamma}{\pi^3}U_v^2\omega_v^2\tau'' & \omega_v^2 - \frac{\gamma}{\pi^3}U_v^2\omega_v^2\beta'' \end{pmatrix}.$$

Natural frequencies and modal damping for coupled vibration can be calculated from eigenvalues of Eq. 15 with $p = 0$.

5. Fluid-Damping Controlled Instability

When one of the tubes is allowed to oscillate in a specific direction while the other tubes are rigid, the equations of motion can be simplified significantly. For example, when a tube oscillates in the x direction, its equation of motion based on Eq. 12 becomes

$$\frac{d^2a}{dt^2} + 2\zeta\omega\frac{da}{dt} + \omega^2 a = \frac{g}{1+\gamma\alpha}, \tag{17}$$

where

$$\omega = \omega_v (1+\gamma C_M)^{-0.5},$$

$$\zeta = \frac{\zeta_v}{1+\gamma\alpha}\left[(1+\gamma C_M)^{0.5} - \frac{\gamma U_r^2 \alpha'}{2\zeta_v \pi^3}\right], \tag{18}$$

$$C_M = \alpha + \frac{U_r^2 \alpha''}{\pi^3}.$$

Note that ω and ζ are the circular frequency and modal damping ratio, respectively, for the tube in crossflow. C_M is called an added mass coefficient for the tube in flow; when $U_r = 0$, it is equal to α_{jj}. When U_r is not equal to zero, C_M depends on U_r as well as on α'', which in turn, depends on U_r and oscillation amplitude.

From Eqs. 17 it is noted that when α' is positive, it will contribute to negative damping to the system. In some cases, the resultant damping may become zero and the system will become unstable. From Eq. 18 the critical reduced flow velocity at which the modal damping ratio is zero can be calculated from

$$U_r = 4\sqrt{2\pi}\left(\frac{\delta}{\alpha'}\right)^{0.5}\left[\frac{\delta}{\pi^2}\left(\frac{\alpha''}{\alpha'}\right) \pm \sqrt{\left(\frac{\delta}{\pi^3}\right)^2 + \frac{1+\gamma\alpha}{4}}\right]^{0.5}, \tag{19}$$

where δ is a mass-damping parameter ($\delta = 2\pi\zeta_v m/\rho D^2$). This is the critical flow velocity for fluidelastic instability.

Equations 17-19 can also be applied to oscillations in the y direction. Replacing all α by β in Eqs. 17-19 yields the equations of motion and stability criterion for constrained mode in the y direction. From Eqs. 17 and 18, it is noted that when the value of the fluid-damping coefficient, α' or β', is positive, the tube may become unstable. The region depends on tube arrangement, location, and flow velocity. From the fluid-force coefficients, α' is found to be positive in a region at lower reduced flow velocity for all cases..

6. Conclusions

The unsteady flow theory has been used extensively in the aerospace industry. In this paper, a direct-measurement technique for fluid damping and fluid stiffness is a convenient way to characterize the fluid effects on tube vibration in cross flow. Similar data have been used successfully in the prediction of fluidelastic instability and chaotic vibration of tube arrays in steam generators (Tanaka and Takahara 1981; Chen 1983a, 1983b; Chen, Zhu, and Cai 1994).

Fluid-force coefficients depend on tube arrangement, pitch, oscillation amplitude, reduced flow velocity, and Reynolds number. At high reduced flow velocity and Reynolds number, fluid-force coefficients are practically independent of reduced flow velocity and oscillation amplitude. Therefore, the mathematical model for the coupled flow-tube systems is simpler at higher reduced flow velocity.

Once fluid damping and fluid stiffness are know, the response of tubes in crossflow can be predicted on the basis of the unsteady flow theory. Tube response characteristics depend on the fluid damping and fluid stiffness. The system may become unstable due to fluid damping or fluid stiffness. For a constrained mode in the lift direction, the fluid-damping-controlled instability can occur at lower reduced flow velocity.

Acknowledgment

This work was funded by the U. S. Department of Energy, Office of Basic Energy Sciences, Division of Engineering and Geosciences, under Contract W-31-109-Eng-38.

References

Cai, Y., and Chen, S. S. 1993. "Chaotic Vibration of Nonlinearly Supported Tubes in Crossflow." J. Pressure Vessel Technology, Vol. 115, pp. 128-134.

Chen, S. S. 1975. "Vibration of Nuclear Fuel Bundles." Nucl. Eng. Des., Vol. 25, pp. 413-431.

Chen, S. S. 1983a. "Instability Mechanism and Stability Criteria of a Group of Circular Cylinders Subjected to Crossflow. Part 1: Theory." J. of Vibration, Acoustics, Stress and Reliability in Design, Vol. 105, pp. 51-58.

Chen, S. S. 1983b. "Instability Mechanism and Stability Criteria of a Group of Circular Cylinders Subjected to Crossflow. Part II: Numerical Results and Discussions." J. of Vibration, Acoustics, Stress and Reliability in Design, Vol. 105, pp. 253-260.

Chen, S. S. 1987. Flow-Induced Vibration of Circular Cylindrical Structures. Hemisphere Publishing Co., New York.

Chen, S. S., and Chandra, S. 1991. "Fluidelastic Instabilities in Tube Bundles Exposed to Nonuniform Cross-Flow." Journal of Fluids and Structures, Vol. 5, pp. 299-322.

Chen, S. S., Zhu, S., and Cai, Y. 1994. "Fluid-Damping-Controlled Instability of Loosely Supported Tube Arrays in Crossflow." ASME Publication, PVP-Vol. 273, pp. 99-115.

Chen, S. S., Zhu, S., and Jendrzejczyk, J. A. 1994. "Fluid Damping and Fluid Stiffness of a Tube Row in Crossflow." ASME Publication, PVP-Vol. 273, pp. 15-31.

Price S. J. 1993. "Theoretical Models of Fluidelastic Instability for Cylinder Arrays Subject to Cross Flow." in Technology for the '90s, ASME Publication, Ed. M. K. Au-Yang, pp. 711-773.

Tanaka, H., and Takahara, S. 1981. "Fluid Elastic Vibration of Tube Array on Cross Flow." Journal of Sound and Vibration, Vol. 77(1), pp. 19-37.

Figure Captions

1. Circular tube oscillating in crossflow

2. Tube arrangements: (a) a single tube; (b) two tubes in tandem, P = 1.35 D; (c) a tube in the wake of another tube; (d) two tube normal to flow, T = 1.35 D; (e) a tube row, T/D = 2.7; and (f) a tube row , T/D = 1.35

3. Fluid-stiffness and fluid-damping coefficients for a single tube, U = 0.127 m/s

4. Fluid-stiffness and fluid-damping coefficients for two tubes in tandem

5. Fluid-stiffness and fluid-damping coefficients for a tube in the wake of another, P/D = 2.70 and T/D = 1.35

6. Fluid-stiffness and fluid-damping coefficients for a tube in the wake of another, P/D = 4.05 and T/D = 1.35

7. Fluid-stiffness and fluid-damping coefficients for a tube in the wake of another, P/D = 4.05 and T/D = 2.70

8. Fluid-stiffness and fluid-damping coefficients for two tubes normal to flow

9. Fluid-stiffness and fluid-damping coefficients for a tube row, T/D = 2.70

10. Fluid-stiffness and fluid-damping coefficients for a tube row, T/D = 1.35

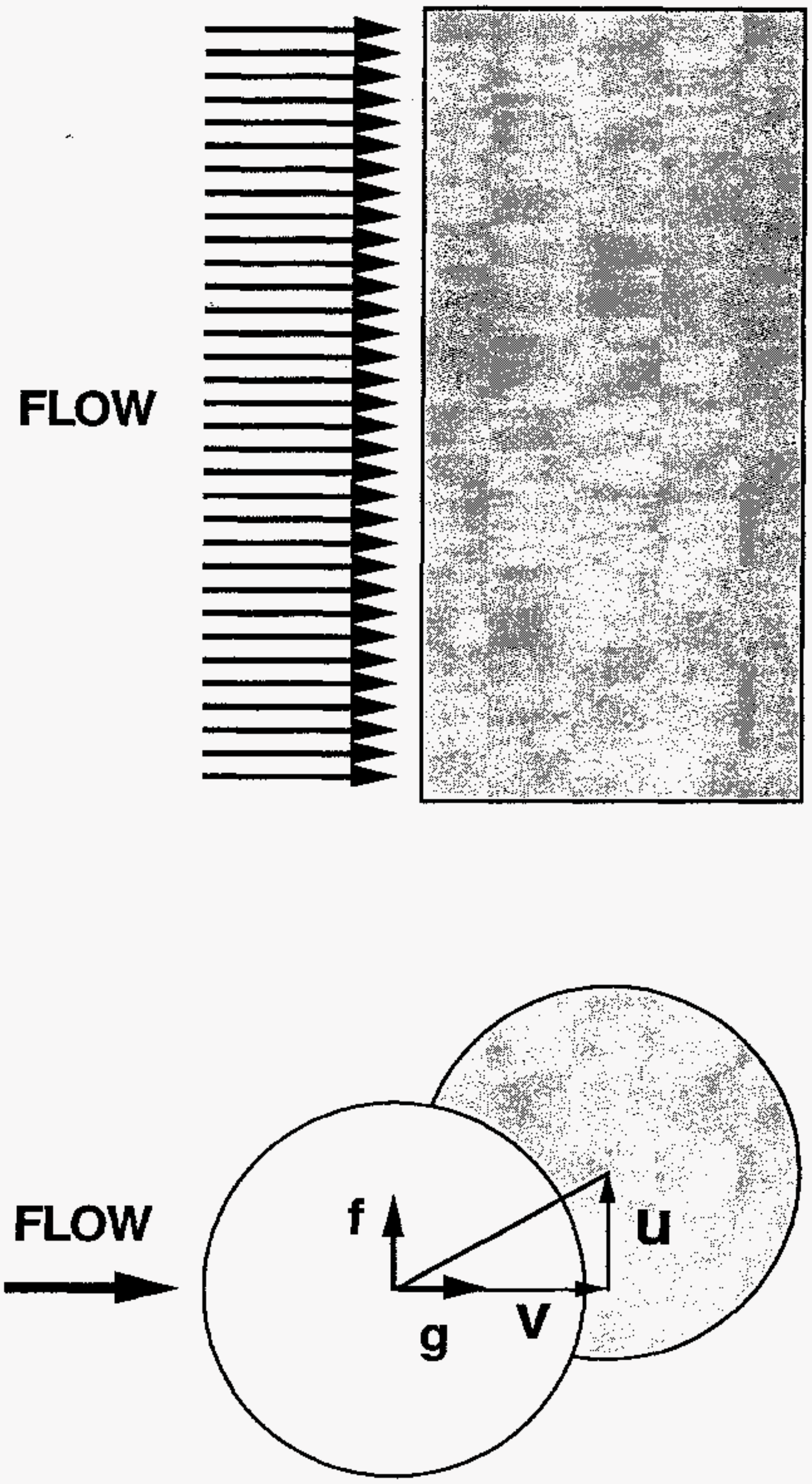

Fig. 1

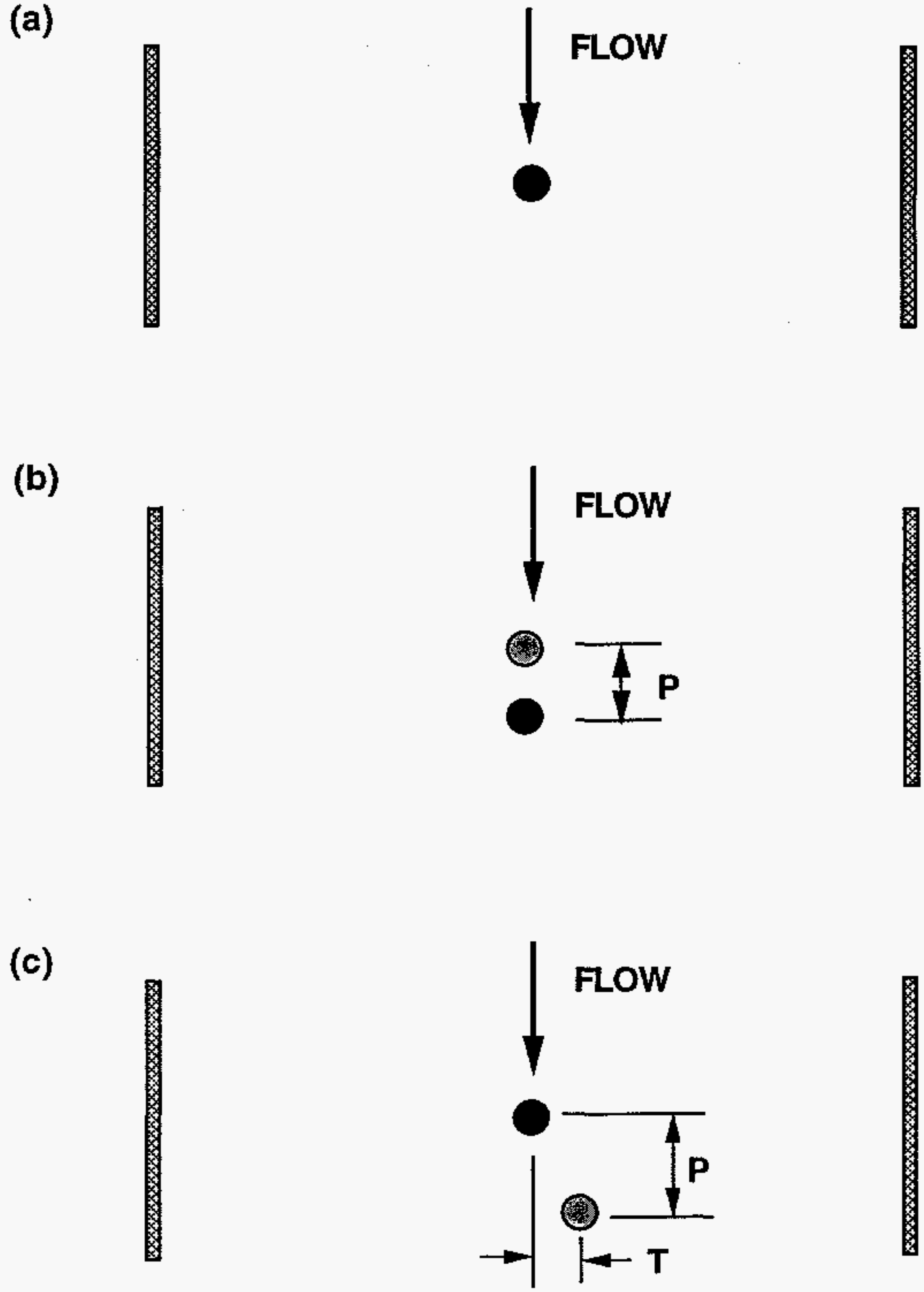

Fig. 2

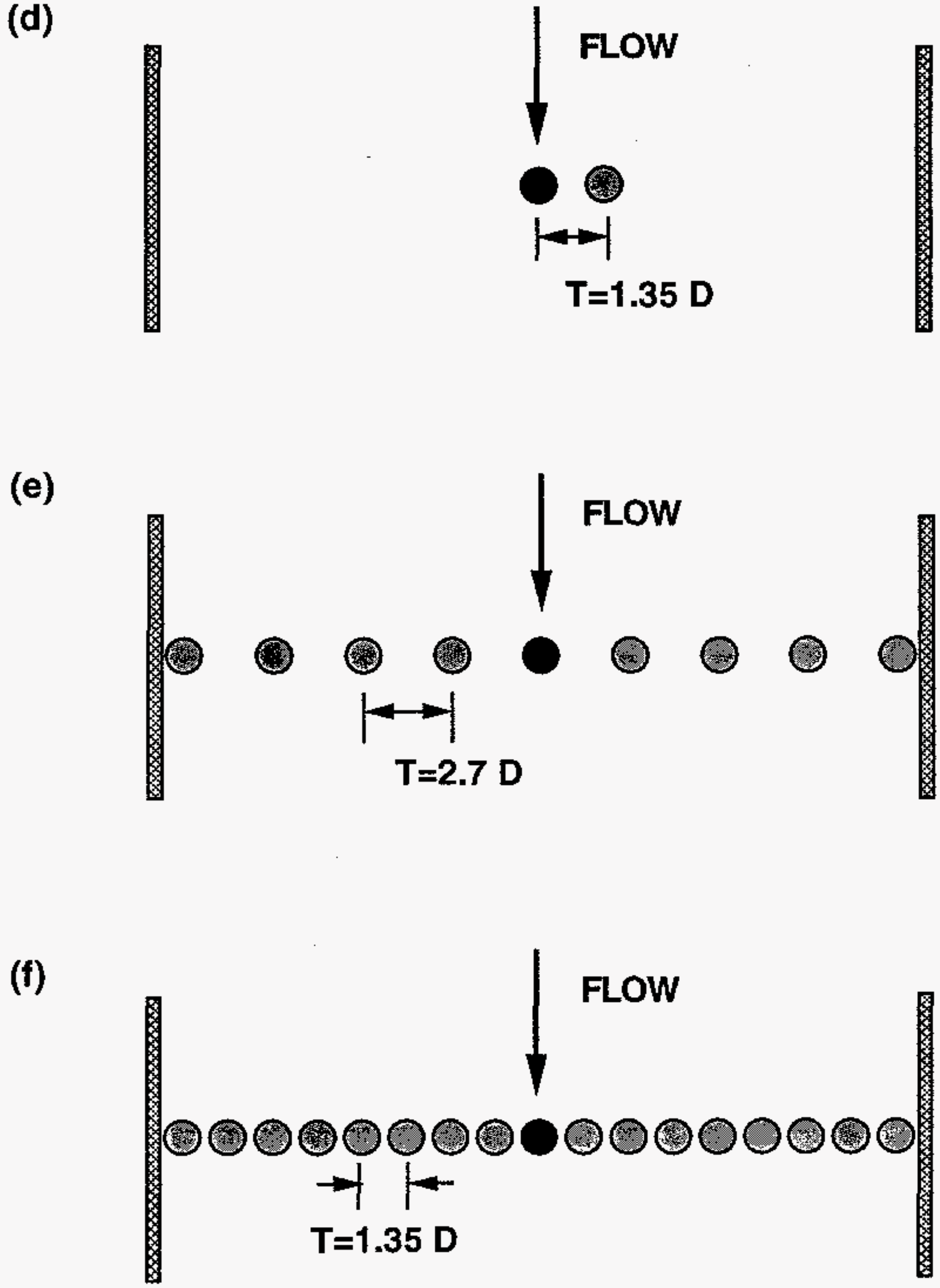

Fig. 2
Con T'd

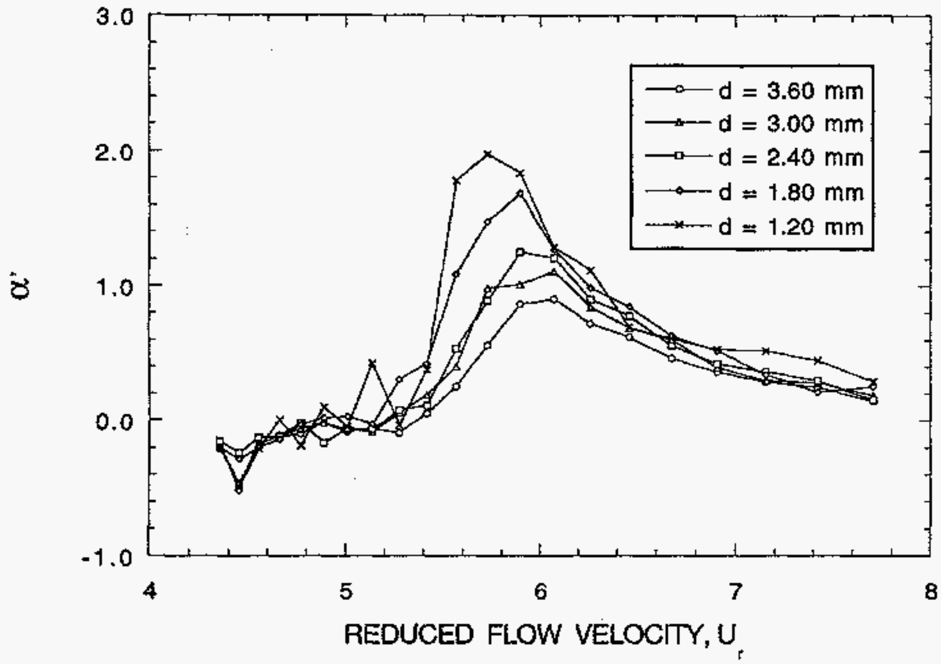

3.0
2.0
1.0
0.0
-1.0
α'
d = 3.60 mm
d = 3.00 mm
d = 2.40 mm
d = 1.80 mm
d = 1.20 mm
4
5
6
7
8
REDUCED FLOW VELOCITY, U r

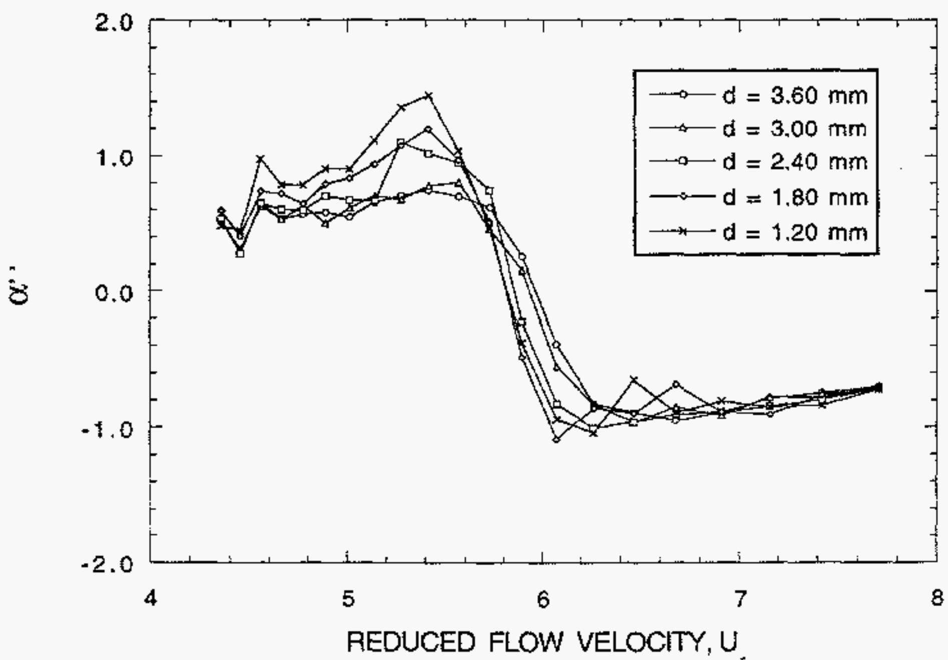

2.0
1.0
0.0
-1.0
-2.0
α''
d = 3.60 mm
d = 3.00 mm
d = 2.40 mm
d = 1.80 mm
d = 1.20 mm
4
5
6
7
8
REDUCED FLOW VELOCITY, U r

Fig. 3

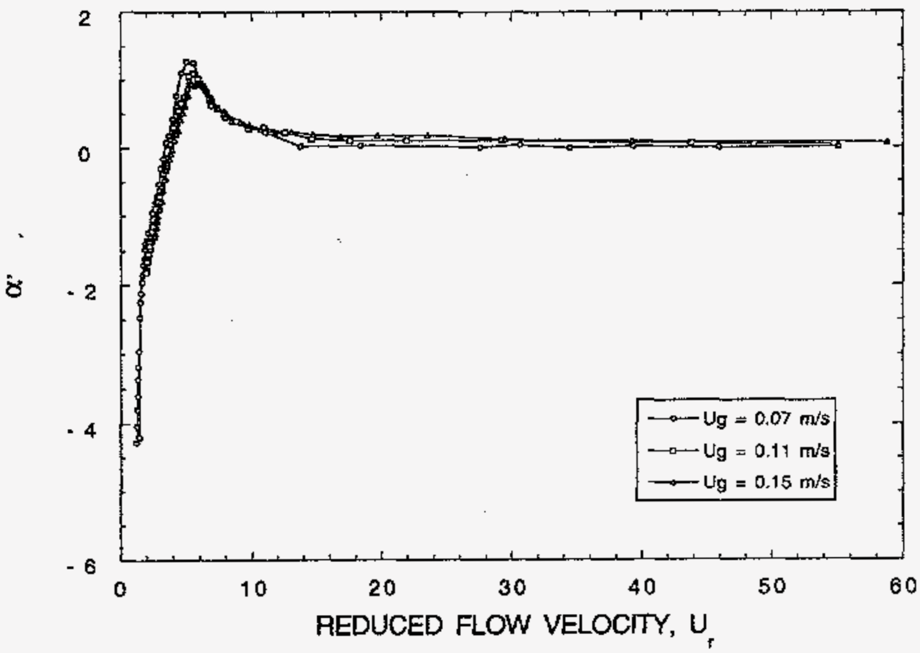
2
0
-2
-4
-6
α'
Ug = 0.07 m/s
Ug = 0.11 m/s
Ug = 0.15 m/s
0
10
20
30
40
50
60
REDUCED FLOW VELOCITY, U_r

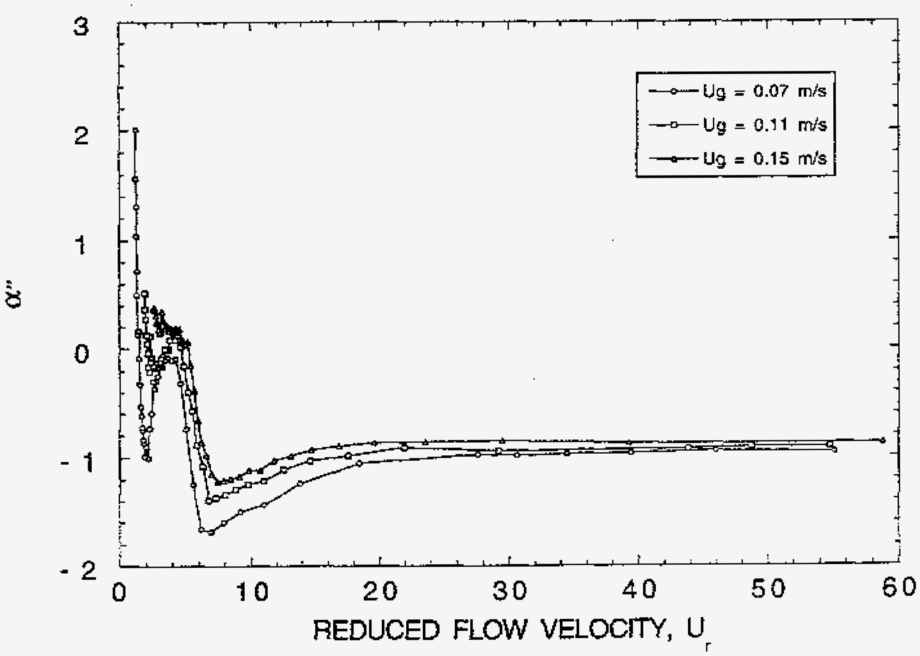
3
2
1
0
-1
-2
α"
Ug = 0.07 m/s
Ug = 0.11 m/s
Ug = 0.15 m/s
0
10
20
30
40
50
60
REDUCED FLOW VELOCITY, U_r

Fig 4

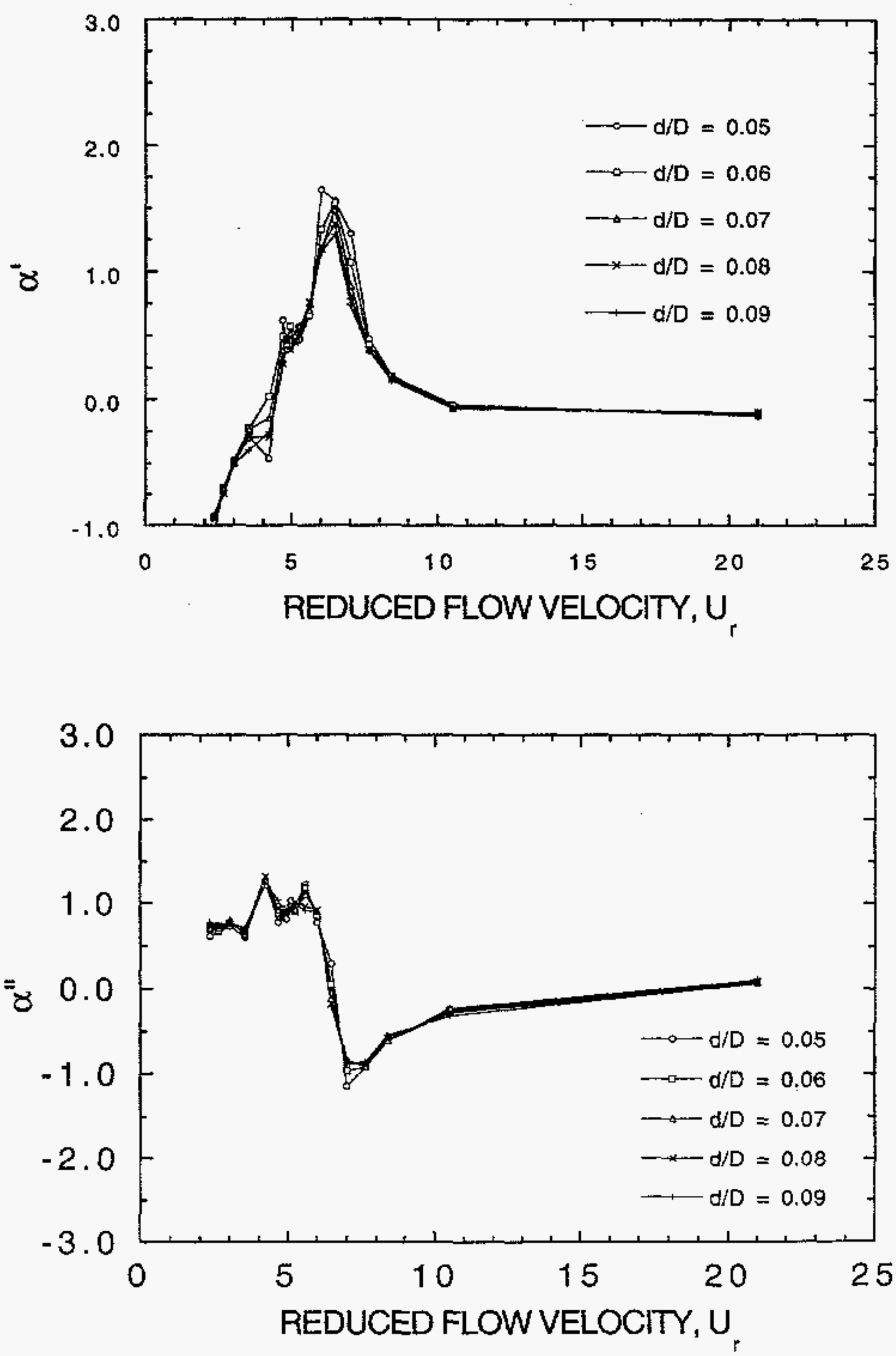
3.0
2.0
1.0
0.0
-1.0
α'
d/D = 0.05
d/D = 0.06
d/D = 0.07
d/D = 0.08
d/D = 0.09
0
5
10
15
20
25
REDUCED FLOW VELOCITY, U_r
3.0
2.0
1.0
0.0
-1.0
-2.0
-3.0
α''
d/D = 0.05
d/D = 0.06
d/D = 0.07
d/D = 0.08
d/D = 0.09
0
5
10
15
20
25
REDUCED FLOW VELOCITY, U_r

Fig. 5

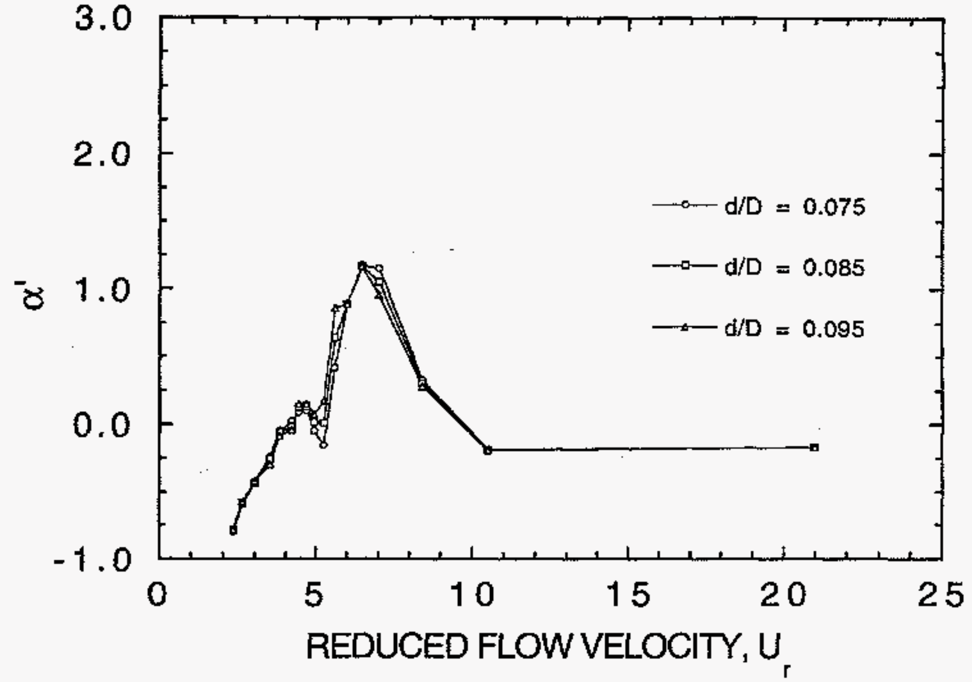
3.0
2.0
1.0
0.0
-1.0
α'
d/D = 0.075
d/D = 0.085
d/D = 0.095
0
5
10
15
20
25
REDUCED FLOW VELOCITY, U
r

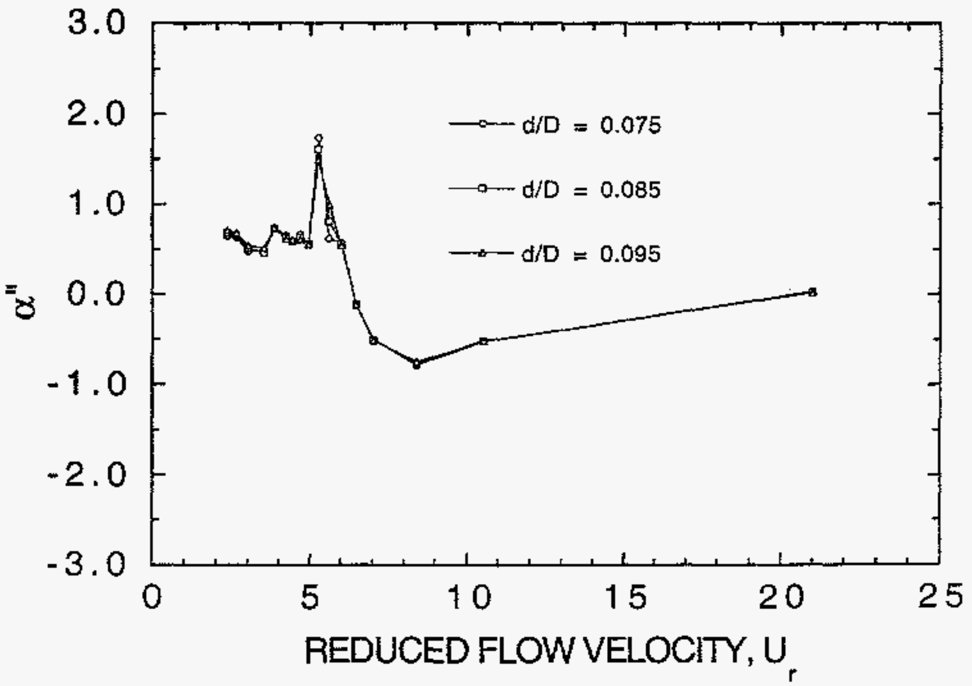
3.0
2.0
1.0
0.0
-1.0
-2.0
-3.0
α"
d/D = 0.075
d/D = 0.085
d/D = 0.095
0
5
10
15
20
25
REDUCED FLOW VELOCITY, U
r

Fig 6

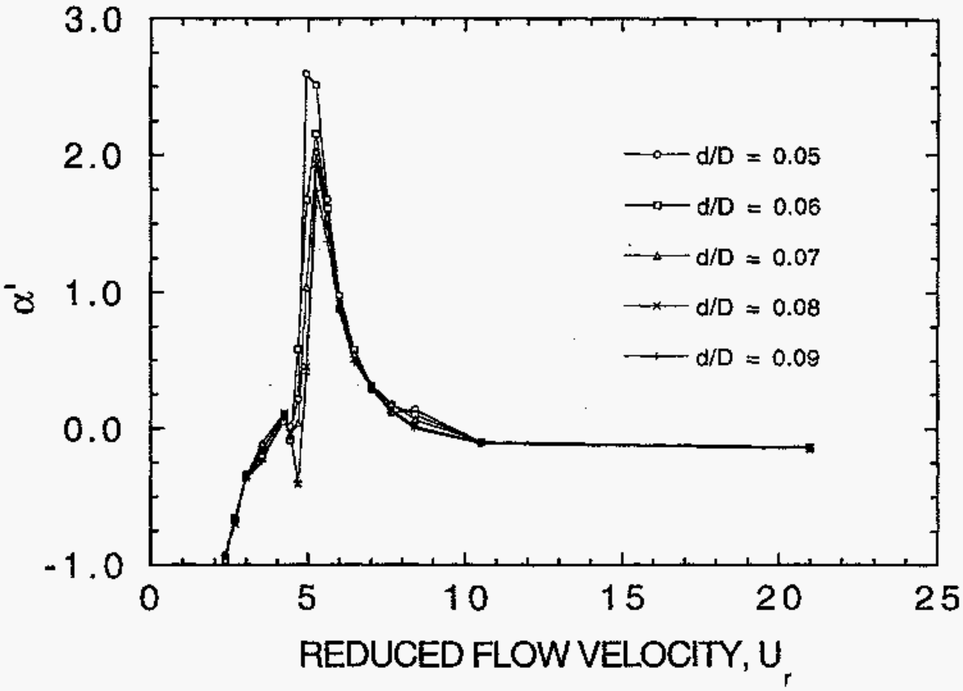

3.0
2.0
1.0
0.0
-1.0
α'
d/D = 0.05
d/D = 0.06
d/D = 0.07
d/D = 0.08
d/D = 0.09
0
5
10
15
20
25
REDUCED FLOW VELOCITY, U_r

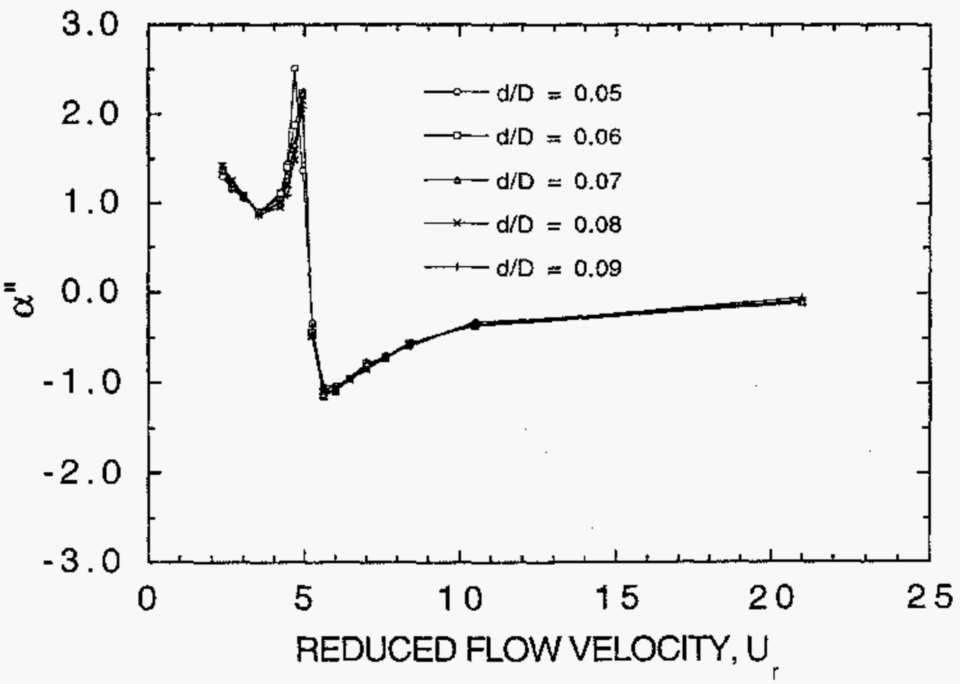

3.0
2.0
1.0
0.0
-1.0
-2.0
-3.0
α''
d/D = 0.05
d/D = 0.06
d/D = 0.07
d/D = 0.08
d/D = 0.09
0
5
10
15
20
25
REDUCED FLOW VELOCITY, U_r

Fig. 7

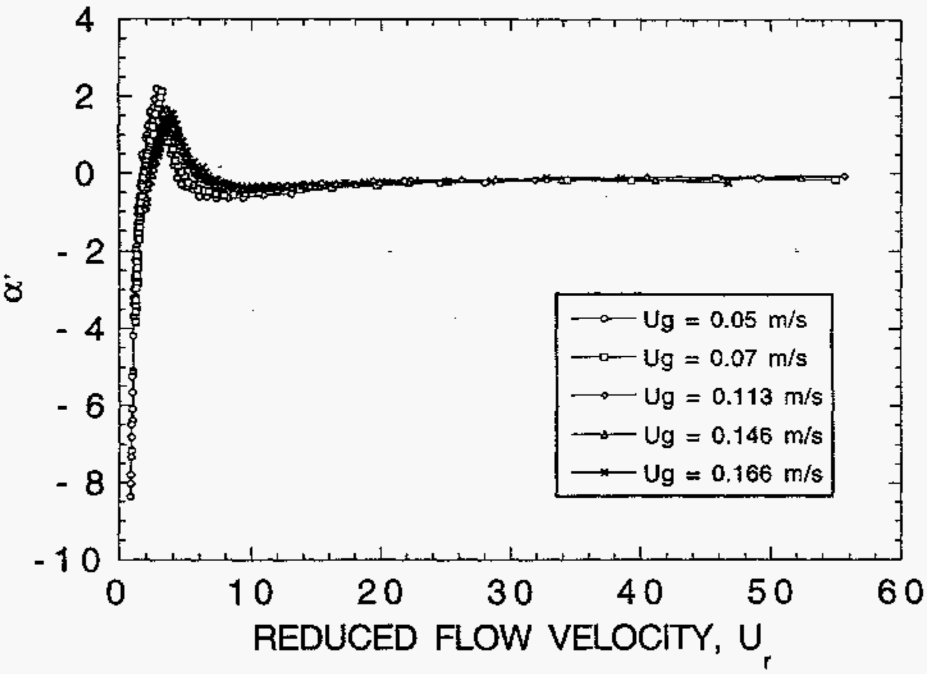
α'
REDUCED FLOW VELOCITY, U_r
Ug = 0.05 m/s
Ug = 0.07 m/s
Ug = 0.113 m/s
Ug = 0.146 m/s
Ug = 0.166 m/s

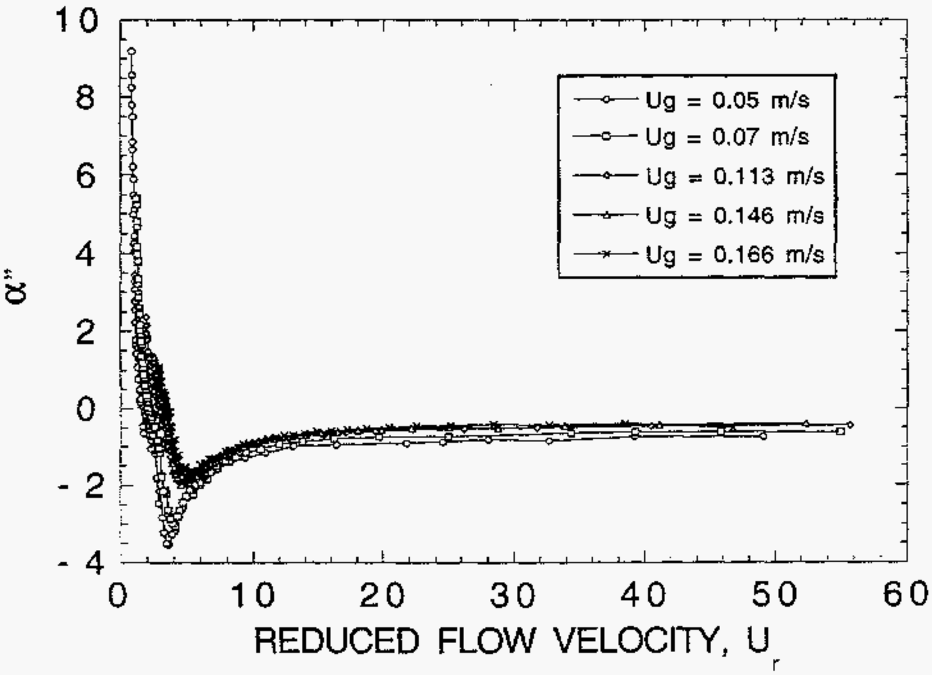
α"
REDUCED FLOW VELOCITY, U_r
Ug = 0.05 m/s
Ug = 0.07 m/s
Ug = 0.113 m/s
Ug = 0.146 m/s
Ug = 0.166 m/s

7.8

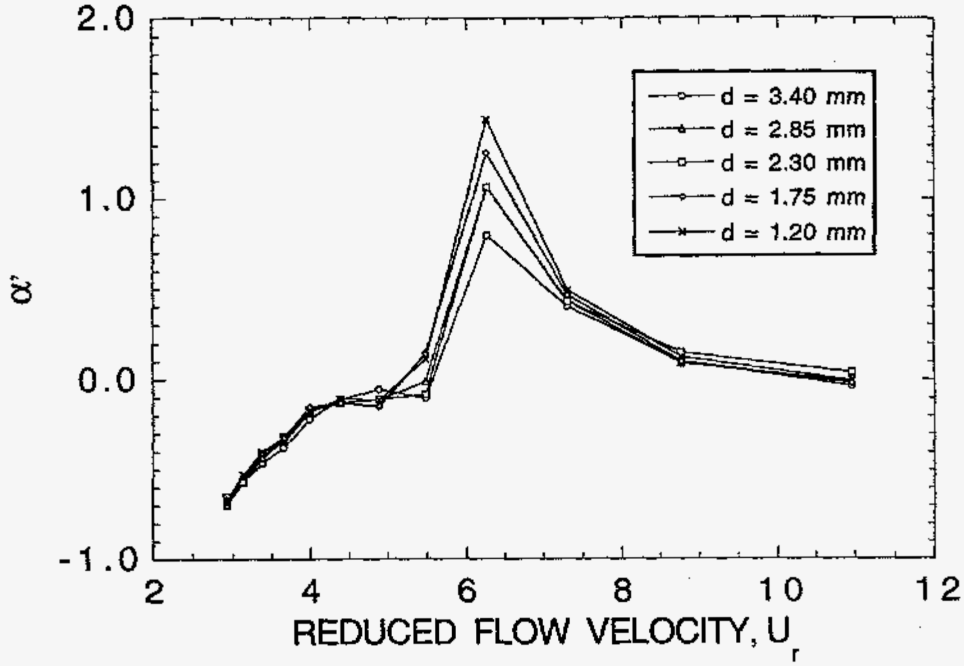
2.0
1.0
0.0
-1.0
α'
2
4
6
8
10
12
REDUCED FLOW VELOCITY, U_r
d = 3.40 mm
d = 2.85 mm
d = 2.30 mm
d = 1.75 mm
d = 1.20 mm

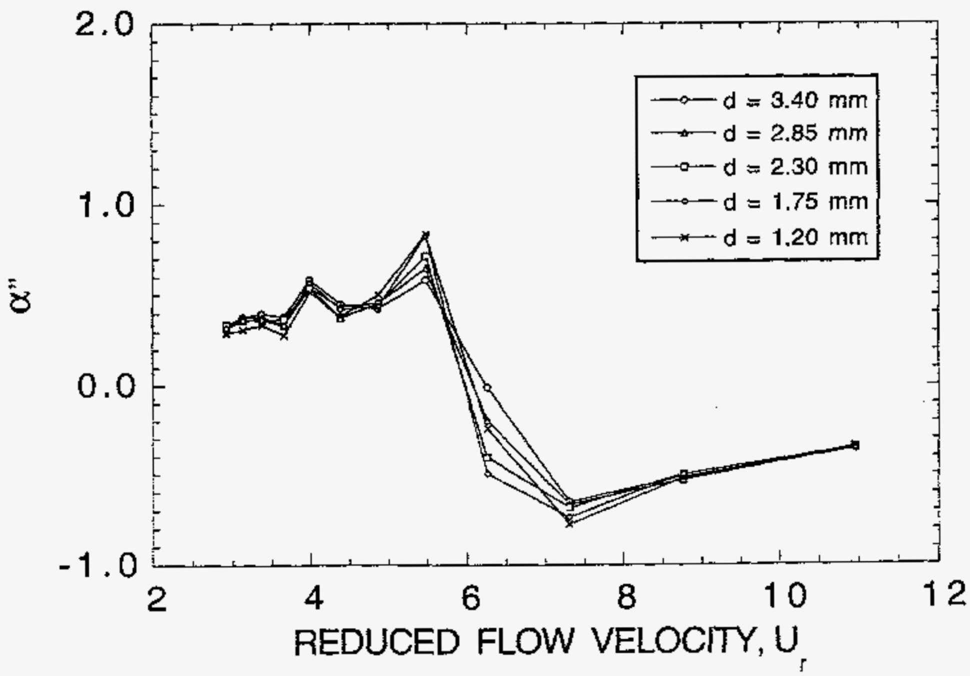
2.0
1.0
0.0
-1.0
α''
2
4
6
8
10
12
REDUCED FLOW VELOCITY, U_r
d = 3.40 mm
d = 2.85 mm
d = 2.30 mm
d = 1.75 mm
d = 1.20 mm

27. 9

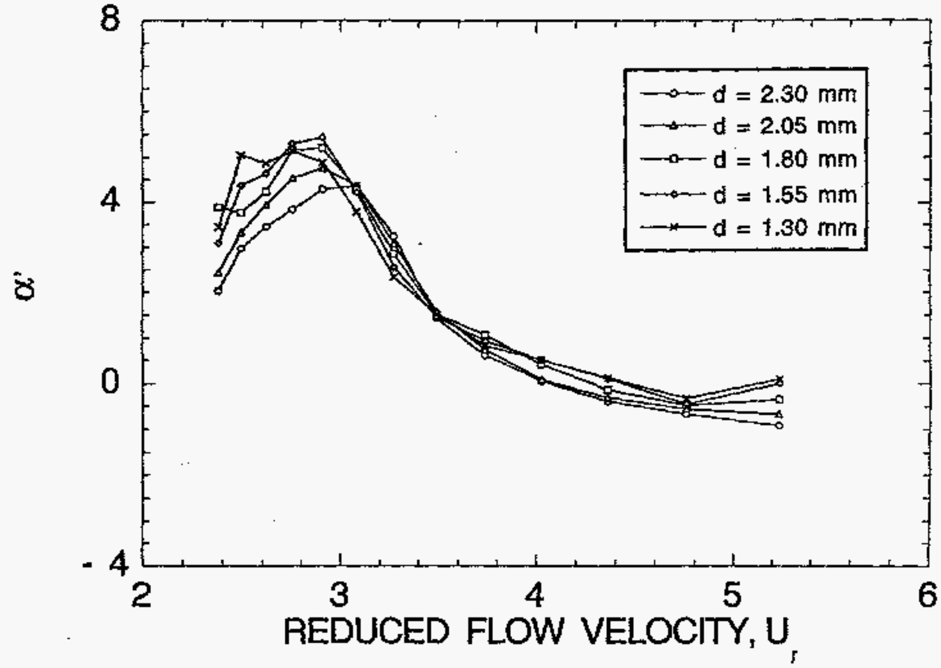

8
4
0
- 4
2
3
4
5
6
α'
d = 2.30 mm
d = 2.05 mm
d = 1.80 mm
d = 1.55 mm
d = 1.30 mm
REDUCED FLOW VELOCITY, U_r

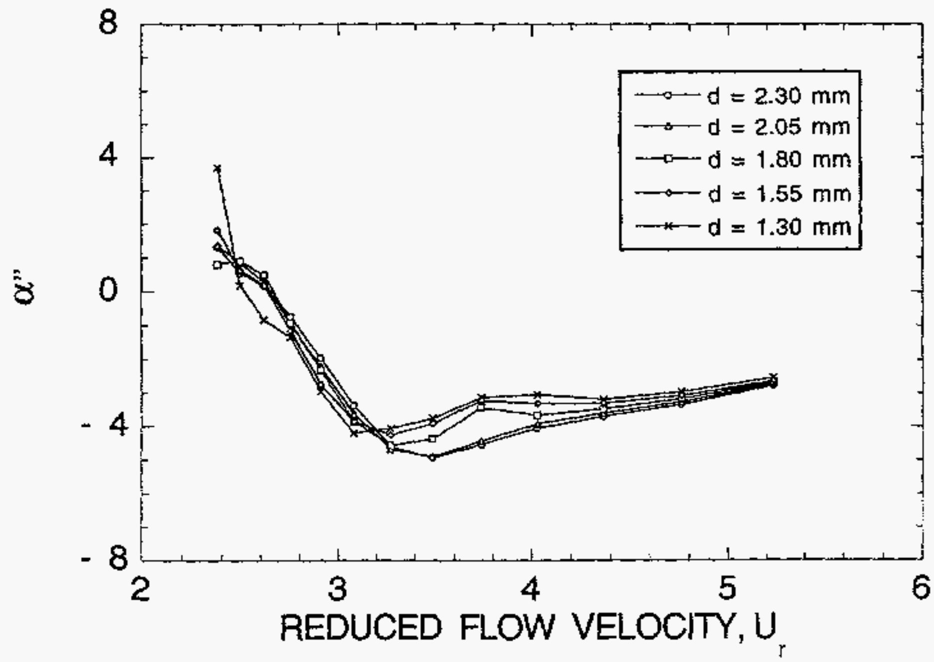

8
4
0
- 4
- 8
2
3
4
5
6
α"
d = 2.30 mm
d = 2.05 mm
d = 1.80 mm
d = 1.55 mm
d = 1.30 mm
REDUCED FLOW VELOCITY, U_r

Fig. 10